



OPEN

Comparison of the incidence of slow flow after rotational atherectomy with IVUS-crossable versus IVUS-uncrossable calcified lesions

Kenichi Sakakura , Yousuke Taniguchi, Kei Yamamoto, Takunori Tsukui, Masaru Seguchi, Hiroshi Wada, Shin-ichi Momomura & Hideo Fujita

Although the usefulness of intravascular ultrasound (IVUS) in rotational atherectomy (RA) has been widely recognized, an IVUS catheter may not cross the target lesion because of severe calcification. The aim of this study was to compare the incidence of slow flow following RA between IVUS-crossable versus IVUS-uncrossable calcified lesions. We included 284 RA lesions, and divided into an IVUS-crossable group ($n = 150$) and an IVUS-uncrossable group ($n = 134$). The primary endpoint was slow flow just after RA. The incidence of slow flow (TIMI flow grade ≤ 2) was significantly greater in the IVUS-uncrossable group than in the IVUS-crossable group (26.1% vs. 10.7%, $p = 0.001$). The incidence of severe slow flow (TIMI grade ≤ 1) was also greater in the IVUS-uncrossable group than in the IVUS-crossable group (9.7% vs. 2.7%, $p = 0.022$). The multivariate logistic regression model showed a significant association between slow flow and pre-IVUS uncrossed lesions (vs. crossed lesions: odds ratio 2.103, 95% confidence interval 1.047–4.225, $p = 0.037$). In conclusion, the incidence of slow flow/severe slow flow just after RA was significantly greater in the IVUS-uncrossable lesions than in the IVUS-crossable lesions. Our study suggests the possibility that the IVUS-crossability can be used as a risk stratification of severe calcified lesions.

Rotational atherectomy (RA) is still a cornerstone for the treatment of coronary lesions with a high calcium content¹. However, the incidence of severe complications is greater in percutaneous coronary interventions (PCI) with than without RA², demanding further refinement in RA. Intravascular imaging devices including intravascular ultrasound (IVUS) and optical coherence tomography (OCT) can provide useful information regarding calcification such as depth, longitudinal length, and arch of calcification^{3–6}. Therefore, intravascular imaging devices have been frequently used in current PCI with RA^{7–9}. Moreover, the intravascular imaging may be helpful in the selection of initial burr sizes or RotaWires (BOSTON SCIENTIFIC, Marlborough, MA, USA), especially for operators with insufficient experiences in RA¹⁰.

Although the usefulness of intravascular imaging devices in RA has been widely recognized, an intravascular imaging device may not cross the target lesion because of severe calcification¹¹. If an IVUS catheter cannot cross the lesion, operators have to decide the strategy of RA from angiographic findings by their own experiences, which may be a difficult situation for junior RA operators. Furthermore, if the incidence of complications following RA was greater in the IVUS-uncrossable lesions than in the IVUS-crossable lesions, junior RA operators would face high-risk lesions without imaging information, which could result in fatal complications. The aim of this study was to compare the incidence of slow flow following RA between IVUS-crossable versus IVUS-uncrossable calcified lesions.

Division of Cardiovascular Medicine, Saitama Medical Center, Jichi Medical University, 1-847 Amanuma, Omiya, Saitama 330-8503, Japan. ✉ email: ksakakura@jichi.ac.jp

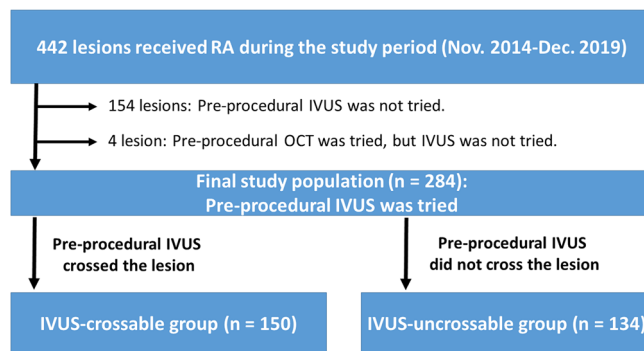


Figure 1. Study flow chart. RA rotational atherectomy, IVUS intravascular ultrasound, OCT optical coherence tomography.

Methods

Study design. This was a retrospective, single-center study. We reviewed 442 consecutive coronary lesions that were treated by RA in our institution during the period from November 2014 to December 2019. Indications for RA in our institution are the following: (1) angiographically moderate or severely calcified lesions, (2) diffuse lesions expected to be difficult to stent, and (3) ostial lesions^{12,13}. We excluded 154 lesions in which pre-procedural IVUS was not attempted, and also excluded 4 lesions in which pre-procedural OCT was attempted but pre-procedural IVUS was not attempted. The final study consisted of 284 lesions, in which pre-procedural IVUS catheter was attempted before RA. The lesions were further classified into an IVUS-crossable group (n = 150) and an IVUS-uncrossable group (n = 134) according to the pre-procedural IVUS-crossability. The study flow chart is shown in Fig. 1. The primary endpoint was slow flow defined as transient thrombolysis in myocardial infarction (TIMI) flow grade ≤ 2 just after RA¹⁴. The secondary endpoint was severe slow flow defined as transient TIMI flow grade ≤ 1 just after RA. We also compared the incidence of ischemia-driven target vessel revascularization (TVR) between the 2 groups. The study was approved by the institutional review board of the Saitama Medical Center, Jichi Medical University, and written informed consent was waived by the institutional review board of the Saitama Medical Center, Jichi Medical University, because of the retrospective study design. All methods were performed in accordance with the relevant guidelines and regulations.

Acquisition of angiograms and evaluation of slow flow. The procedures were performed with a biplane fluoroscopy system [Artis zee BC (Model number 10094141, Model year 2009, March) and Artis zee BA (Model number 10094141, Model year 2013, January), SIEMENS, Munich, Germany] containing three magnetic fields and a standard image acquisition program at 15 frames per second during cine acquisition and 7.5 frames per second during fluoroscopy¹⁵. Thus, the evaluation of slow flow was done at 15 frames per second. Operators used a power injector (Zone master, Suga Co., Ltd., Osaka, Japan) with predefined settings (total 7 ml, 3 ml/s for left coronary artery, total 5 ml, 2.5 ml/s for right coronary artery). However, operators modified the amount of contrast and injection speed to achieve sufficient images. The evaluation of TIMI-flow grade just after RA was performed by an unblinded operator (KS) like previous studies regarding RA from our institution^{12–14,16}.

Rotational atherectomy. RA was performed using standard techniques as previously described¹¹. A nicorandil-based drug cocktail was used during RA to prevent slow flow¹⁷. We preferred to use ≥ 7 -Fr guide catheters with side holes for RA. The lesion was crossed with a 0.014-inch conventional guidewire, and IVUS was attempted. The type of IVUS catheter was selected based on the discretion of the interventional cardiologist. Among 284 lesions, OptiCross (n = 222) (BOSTON SCIENTIFIC, Marlborough, MA, USA), Navifocus WR (n = 43) (TERUMO, Tokyo, Japan), AltaView (n = 15) (TERUMO, Tokyo, Japan), Eagle Eye (n = 3) (PHILLIPS VOLCANO, San Diego, CA, USA), and ViewIT (TERUMO, Tokyo, Japan) (n = 1) were used as the IVUS catheter. After the attempt of IVUS, a 0.014-inch conventional guidewire was exchanged with a 0.009-inch RotaWire floppy or RotaWire extra support guidewire (BOSTON SCIENTIFIC, Marlborough, MA, USA) using a micro-catheter. The RA burr was subsequently advanced over the wire to a position proximal to the lesion. The initial rotational speed was set within the conventional range (140,000–190,000 rpm) with the burr proximal to the lesion, and several lesions were randomly allocated to 140,000 rpm or 190,000 rpm¹³. The burr was activated and moved forward with a slow pecking motion. Each run time was < 30 s, and care was taken to avoid a decrease in rotational speed $> 5,000$ rpm. However, the excessive speed down was sometimes observed especially in the ostium of right coronary artery¹⁶. The initial burr size was either 1.25-mm or 1.5-mm, which is supported by the European expert consensus on RA¹⁸. After the burr passed the lesion, the burr was removed using the dynaglide mode or trapping balloon technique¹⁹. The presence of coronary flow was confirmed by injecting sufficient contrast medium immediately after the burr was removed. Following RA, balloon dilatation was performed using a non-compliant balloon/scoring balloon/cutting balloon to facilitate stent implantation.

RA was not used as first-line therapy to treat culprit lesions in acute coronary syndrome (ACS); however, RA was used to treat culprit lesions in ACS if necessary¹⁴. Furthermore, an intra-aortic balloon pump (IABP) was inserted via a femoral artery before RA in high-risk cases such as those with severe left ventricular dysfunction,

unprotected left main stenosis, or severe 3-vessel disease¹¹. This was done because complications such as slow flow or peri-procedural myocardial infarction were more frequent in these high-risk cases¹².

Complications. We collected data on the following complications: slow flow just after RA, severe slow flow just after RA, vessel perforation (type III) due to the burr, burr entrapment, and peri-procedural myocardial infarction with slow flow. Peri-procedural myocardial infarction was defined as an increase in creatine kinase (at least three-fold above the normal upper limit)^{12,13}.

Definitions. Hypertension was defined as a systolic blood pressure >140 mmHg, diastolic blood pressure >90 mmHg, or medical treatment for hypertension¹³. Diabetes mellitus was defined as a hemoglobin A1c level >6.5% or treatment for diabetes mellitus^{13,20}. Hyperlipidemia was defined as a total cholesterol level >220 mg/dl, a low-density lipoprotein cholesterol level >140 mg/dl, or treatment for hyperlipidemia¹³. eGFR was calculated using the MDRD formula²¹. ACS was defined as ST-segment elevation myocardial infarction, non-ST-segment elevation myocardial infarction, or unstable angina¹³. The reference diameter and lesion length were calculated by quantitative coronary angiography. Offline, computer-based software QAngio XA 7.3 (MEDIS Imaging Systems, Leiden, The Netherlands) was used for quantitative coronary angiography¹¹. The burr-to-artery ratio was defined as the burr size divided by the reference diameter¹¹.

Statistical analysis. Data are presented as a percentage for categorical variables and the mean \pm SD for continuous variables. The Wilk–Shapiro test was performed to determine if the continuous variables were normally distributed. Normally distributed continuous variables were compared between the 2 groups using a Student's *t* test. Otherwise, continuous variables were compared using a Mann–Whitney *U* test. Categorical data were compared using a Fischer's exact test. We performed multivariate stepwise logistic regression analysis to investigate the association between IVUS-crossability and slow flow. In the model 1, the dependent variable was slow flow just after RA. Variables that had a significant association ($P < 0.05$) between the 2 groups were used as independent variables. The multivariate logistic regression analysis with Wald Statistical criteria using backward elimination method was performed. In the model 2, the dependent variable was severe slow flow just after RA. Variables that had a significant association ($P < 0.05$) between the 2 groups were used as independent variables. The multivariate logistic regression analysis with Wald Statistical criteria using backward elimination method was performed. Odds ratios (OR) and the 95% confidence intervals (CI) were calculated. Ischemia-driven TVR-free survival curves were constructed using the Kaplan–Meier method, and the statistical difference between curves was assessed by the log-rank test. All reported *P*-values were determined by two-sided analysis, and *P*-values <0.05 were considered significant. All analyses were performed with IBM SPSS statistics version 25 (Chicago, IL, USA).

Results

The comparison of patients and lesion characteristics between the 2 groups are summarized in Table 1. The prevalence of male sex was significantly less in the IVUS-uncrossable group than in the IVUS-crossable group (65.7% vs. 76.7%, $p = 0.048$). The prevalence of diabetes mellitus was significantly greater in the IVUS-uncrossable group than in the IVUS-crossable group (65.7% vs. 52.3%, $p = 0.029$). The culprit lesion in acute coronary syndrome was more frequently observed in the IVUS-uncrossable group than in the IVUS-crossable group (26.1% vs. 14.0%, $p = 0.011$). Left main-left anterior descending artery lesions were less frequently observed in the IVUS-uncrossable group than in the IVUS-crossable group ($p = 0.015$). The reference diameter was significantly smaller in the IVUS-uncrossable group than in the IVUS-crossable group (2.26 ± 0.59 mm vs. 2.54 ± 0.61 mm, $p < 0.001$). The lesion length was significantly longer in the IVUS-uncrossable group than in the IVUS-crossable group (27.40 ± 15.65 mm vs. 22.99 ± 15.47 mm, $p = 0.008$). Moderate to severe angulation was more frequently observed in the IVUS-uncrossable group than in the IVUS-crossable group ($p = 0.002$).

The comparison of procedural characteristics between the 2 groups is summarized in Table 2. The guide-wire switch was more frequently performed in the IVUS-uncrossable group than in the IVUS-crossable group ($p = 0.003$). The 1.25-mm burr was more frequently used as an initial burr in the IVUS-uncrossable group than in the IVUS-crossable group (39.6% vs. 15.3%, $p < 0.001$). The final burr size was smaller in the IVUS-uncrossable group than in the IVUS-crossable group ($p < 0.001$). Initial burr-to-artery ratio was significantly greater in the IVUS-uncrossable group than in the IVUS-crossable group (0.66 ± 0.16 vs. 0.61 ± 0.15 , $p = 0.008$). Total run time, single run time, rotational speed, and maximum speed reduction during RA were significantly greater in the IVUS-uncrossable group than in the IVUS-crossable group.

The comparison of complications between the 2 groups is shown in Table 3. The incidence of slow flow just after RA was significantly greater in the IVUS-uncrossable group than in the IVUS-crossable group (26.1% vs. 10.7%, $p = 0.001$). The incidence of severe slow flow just after RA was also greater in the IVUS-uncrossable group than in the IVUS-crossable group (9.7% vs. 2.7%, $p = 0.022$). The incidence of periprocedural MI was not different between the 2 groups.

The multivariate logistic regression models to investigate the association between IVUS crossability and slow flow/severe slow flow are shown in Table 4. In the model 1, the initial model included male sex, diabetes mellitus, culprit lesion in acute coronary syndrome, target lesion (left main- left anterior descending artery vs. others), lesion length, severe angulation, RotaWire floppy as an initial wire, initial burr-to-artery ratio, and pre-IVUS uncrossed lesions (vs. crossed lesions) as independent variables. The final model showed a significant association between slow flow and pre-IVUS uncrossed lesions (vs. crossed lesions: OR 2.103, 95% CI 1.047–4.225, $p = 0.037$). In the model 2, the initial model also included male sex, diabetes mellitus, culprit lesion in acute coronary syndrome, target lesion (left main- left anterior descending artery vs. others), lesion length, severe

	All (n = 284)	IVUS-crossable group (n = 150)	IVUS-uncrossable group (n = 134)	P value
Patient characteristics				
Age (years)	73.9 ± 8.8	74.7 ± 8.0	73.0 ± 9.5	0.176
Men—n, (%)	203 (71.5)	115 (76.7)	88 (65.7)	0.048
Overweight (BMI ≥ 25 kg/m ²)—n, (%)	79 (27.8)	38 (25.3)	41 (30.6)	0.354
Hypertension—n, (%)	274 (96.5)	143 (95.3)	131 (97.8)	0.343
Diabetes mellitus—n, (%) (n = 283)	166 (58.7)	78 (52.3)	88 (65.7)	0.029
Hyperlipidemia—n, (%)	265 (93.3)	139 (92.7)	126 (94.0)	0.813
Current smoker—n, (%) (n = 282)	44 (15.6)	24 (16.0)	20 (15.2)	0.871
Chronic renal failure (creatinine > 2 mg/dl)—n, (%)	73 (25.7)	33 (22.0)	40 (29.9)	0.137
Estimated GFR (ml/min/1.73 m ²)	65.0 ± 40.6	67.0 ± 38.7	62.8 ± 42.6	0.431
Chronic renal failure on hemodialysis—n, (%)	65 (22.9)	32 (21.3)	33 (24.6)	0.572
Statin treatment—n, (%)	262 (92.3)	138 (92.0)	124 (92.5)	1.000
Lesion characteristics				
Culprit lesion in acute coronary syndrome—n, (%)	56 (19.7)	21 (14.0)	35 (26.1)	0.011
In-stent lesion—n, (%)	19 (6.7)	14 (9.3)	5 (3.7)	0.094
Target coronary artery				0.015
Left main- left anterior descending artery—n, (%)	190 (66.9)	111 (74.0)	79 (59.0)	
Left circumflex artery—n, (%)	17 (6.0)	5 (3.3)	12 (9.0)	
Right coronary artery—n, (%)	77 (27.1)	34 (22.7)	43 (32.1)	
Specific target coronary artery				
Ostial left main—n, (%)	2 (0.7)	2 (1.3)	0	0.500
Ostial left anterior descending artery—n, (%)	36 (12.7)	24 (16.0)	12 (9.0)	0.107
Ostial left circumflex artery—n, (%)	4 (1.4)	3 (2.0)	1 (0.7)	0.625
Ostial right coronary artery—n, (%)	23 (8.1)	12 (8.0)	11 (8.2)	1.000
Reference diameter (mm)	2.41 ± 0.61	2.54 ± 0.61	2.26 ± 0.59	<0.001
Lesion length (mm)	25.07 ± 15.68	22.99 ± 15.47	27.40 ± 15.65	0.008
Initial TIMI flow grade 3—n, (%)	252 (88.7)	137 (91.3)	115 (85.8)	0.188
Lesion angle				0.002
Mild angulation (< 30°)	143 (50.4)	88 (58.7)	55 (41.0)	
Moderate angulation (30°–60°)	112 (39.4)	54 (36.0)	58 (43.3)	
Severe angulation (≥ 60°)	29 (10.2)	8 (5.3)	21 (15.7)	
Angiographically severe calcification	278 (97.9)	147 (98.0)	131 (97.8)	1.000

Table 1. Comparison of patients and lesions characteristics between the IVUS-crossable group and IVU-uncrossable group. Data are expressed as the mean ± SD or number (percentage). A Mann–Whitney *U* test was used for continuous variables, and a Fischer’s exact test was used for categorical variables. *GFR* glomerular filtration rate.

angulation, RotaWire floppy as an initial wire, initial burr-to-artery ratio, and pre-IVUS uncrossed lesions (vs. crossed lesions) as independent variables. The final model showed a significant association between severe slow flow and pre-IVUS uncrossed lesions (vs. crossed lesions: OR 3.312, 95% CI 1.036–10.589, $p = 0.043$). Figure 2 shows the Kaplan–Meier curves of ischemia-driven TVR-free survival. The median follow-up duration was 298 days (Q1–Q3: 177–620 days). Ischemia-driven TVR free survival curves were not different between the 2 groups ($p = 0.697$).

Discussion

A total of 284 severely calcified lesions for which pre-procedural IVUS was attempted before RA were included in the present study, and were divided into an IVUS-crossable group ($n = 150$) and a IVUS-uncrossable group ($n = 134$), according to the IVUS-crossability. The incidence of slow flow/severe slow flow just after RA was significantly greater in the IVUS-uncrossable group than in the IVUS-crossable group. The multivariate logistic regression analysis confirmed the significant association between slow flow/severe slow flow and IVUS-crossability. Our results suggest that special attention should be paid to the IVUS-uncrossable lesions to prevent complications following RA.

Recently, many groups rigorously published research articles regarding RA with intravascular imaging devices^{3,4,6–9}. Moreover, several review articles explain the interpretation of intravascular imaging findings in

	All (n = 284)	IVUS-crossable group (n = 150)	IVUS-uncrossable group (n = 134)	P value
Procedural characteristics				
Guiding catheter size and system				0.081
6Fr—n, (%)	4 (1.4)	0 (0)	4 (3.0)	
7Fr—n, (%)	257 (90.5)	136 (90.7)	121 (90.3)	
8Fr—n, (%)	23 (8.1)	14 (9.3)	9 (6.7)	
Intra-aortic balloon pump support—n, (%)	20 (7.0)	11 (7.3)	9 (6.7)	1.000
Any balloon dilatation or try to balloon dilatation before RA—n, (%)	28 (9.9)	11 (7.3)	17 (12.7)	0.163
Guidewire used during rotational atherectomy				0.003
RotaWire floppy—n, (%)	216 (76.1)	122 (81.3)	94 (70.1)	
RotaWire extra support—n, (%)	40 (14.1)	22 (14.7)	18 (13.4)	
Guidewire switch from floppy to extra support—n, (%)	23 (8.1)	6 (4.0)	17 (12.7)	
Guidewire switch from extra support to floppy—n, (%)	5 (1.8)	0 (0)	5 (3.7)	
Number of burrs used	1.2 ± 0.5	1.3 ± 0.5	1.2 ± 0.5	0.554
Initial burr size				<0.001
1.25-mm	76 (26.8)	23 (15.3)	53 (39.6)	
1.5-mm	208 (73.2)	127 (84.7)	81 (60.4)	
Final burr size				<0.001
1.25-mm	66 (23.2)	17 (6.0)	49 (17.3)	
1.5-mm	173 (60.9)	100 (66.7)	73 (54.5)	
1.75-mm	12 (4.2)	8 (5.3)	4 (3.0)	
2.0-mm	33 (11.6)	25 (16.7)	8 (6.0)	
Initial burr-to-artery ratio	0.63 ± 0.16	0.61 ± 0.15	0.66 ± 0.16	0.008
Final burr-to-artery ratio	0.66 ± 0.17	0.65 ± 0.16	0.68 ± 0.18	0.163
Total run time (s)	91.8 ± 73.2	72.8 ± 59.5	115.1 ± 80.6	<0.001
Mean single run time (s)	12.8 ± 3.1	11.9 ± 2.6	13.7 ± 3.4	<0.001
Mean rotational speed (× 1,000 rpm)	173.2 ± 10.1	171.6 ± 10.6	175.0 ± 9.1	0.021
Maximum speed reduction during rotational atherectomy (rpm) (n = 281)	6,630 ± 5,166	6,228 ± 6,007	7,083 ± 3,987	0.001
Systolic blood pressure just before rotational atherectomy (mmHg)	153 ± 27	153 ± 28	153 ± 26	0.919
Diastolic blood pressure just before rotational atherectomy (mmHg)	75 ± 14	76 ± 15	75 ± 13	0.584
Heart rate just before rotational atherectomy (per minute)	71 ± 14	71 ± 12	72 ± 15	0.657
Final procedure				0.441
Rotational atherectomy + balloon including drug-coating balloon—n, (%)	23 (8.1)	15 (10.0)	8 (6.0)	
Rotational atherectomy + bare-metal stent—n, (%)	3 (1.1)	2 (1.3)	1 (0.7)	
Rotational atherectomy + drug-eluting stent—n, (%)	257 (90.5)	133 (88.7)	124 (92.5)	
Rotational atherectomy + covered stent for perforation—n, (%)	1 (0.4)	0 (0)	1 (0.7)	

Table 2. Comparison of procedural characteristics between the IVUS-crossable group and IVU-uncrossable group. Data are expressed as the mean ± SD or number (percentage). A Mann–Whitney *U* test was used for continuous variables, and a Fischer’s exact test was used for categorical variables. *GFR* glomerular filtration rate.

RA to facilitate use of imaging devices in RA^{1,5,10}. However, there are few literatures focusing on the situation when an intravascular imaging device could not cross the severely calcified lesion before RA. As we shown in the present study, a substantial number of severely calcified lesions did not allow intravascular imaging devices to cross the lesion before RA. Furthermore, if we utilize IVUS correctly, the incidence of severe complications has been considered to lower in RA with than without IVUS¹⁰. However, the US National Inpatient Sample data set for the years 2012 to 2014 showed the higher incidence of iatrogenic and cardiac complications in IVUS-assisted atherectomy²², which would include IVUS-uncrossable lesions. It should be important to discuss strategies for

	All (n = 284)	IVUS-crossable group (n = 150)	IVUS-uncrossable group (n = 134)	P value
Slow flow (\leq TIMI-2) just after RA	51 (18.0)	16 (10.7)	35 (26.1)	0.001
Severe slow flow (\leq TIMI-1) just after RA	17 (6.0)	4 (2.7)	13 (9.7)	0.022
Periprocedural MI with slow flow	4 (1.4)	1 (0.7)	3 (2.2)	0.346
Final TIMI flow grade ≤ 2	2 (0.7)	0	2 (1.5)	0.222
Vessel perforation (Type III) due to Burr	1 (0.4)	0 (0)	1 (0.7)	0.472
Burr entrapment	1 (0.4)	1 (0.7)	0 (0)	1.000

Table 3. Comparison of complications between the IVUS-crossable group and IVU-uncrossable group. Data are expressed as the number (percentage). A Fischer's exact test was used to compare the 2 groups. *TIMI* thrombolysis in myocardial infarction.

Dependent variable: Slow flow			
Independent variables	Odds ratio	95% confidence interval	P value
Model 1: Dependent variable: Slow flow (\leq TIMI-2) just after RA			
Lesion length (every 5 mm increase)	1.098	0.987–1.221	0.086
Severe angulation ($\geq 60^\circ$)	2.767	1.088–7.041	0.033
Initial burr-to-artery ratio (every 0.1 increase)	1.581	1.271–1.966	<0.001
Pre-IVUS uncrossed lesions (vs. pre-IVUS crossed lesions)	2.103	1.047–4.225	0.037
Dependent variable: Severe slow flow			
Independent variables	Odds ratio	95% confidence interval	P value
Model 2: Dependent variable: Severe slow flow (\leq TIMI-1) just after RA			
Initial burr-to-artery ratio (every 0.1 increase)	1.392	1.057–1.833	0.018
Pre-IVUS uncrossed lesions (vs. pre-IVUS crossed lesions)	3.312	1.036–10.589	0.043

Table 4. Multivariate stepwise logistic regression model to investigate the association between pre-IVUS crossability and slow flow. The initial model included male sex, diabetes mellitus, culprit lesion in acute coronary syndrome, target lesion (left main- left anterior descending artery vs. others), lesion length, severe angulation, RotaWire floppy as an initial wire, initial burr-to-artery ratio, pre-IVUS uncrossed lesions (vs. crossed lesions). The multivariate logistic regression analysis with Wald Statistical criteria using backward elimination method was performed.

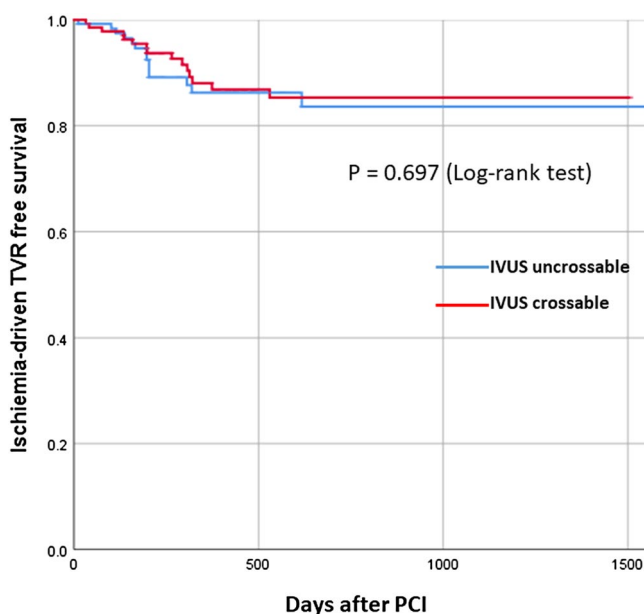


Figure 2. Kaplan–Meier curves of ischemia-driven TVR free survival.

severely calcified lesions that intravascular image devices cannot cross, especially for operators with insufficient RA experiences.

The reason why the incidence of slow flow was greater in the IVUS-uncrossable lesions than in the IVUS-crossable lesions should be discussed. The IVUS-uncrossable group had more complex features such as smaller reference diameter, longer lesion length, and severer angulation. Although the initial burr size was smaller in the IVUS-uncrossable group, initial burr-to-artery ratio was bigger in the IVUS-uncrossable group. Because the longer lesion length or bigger burr-to-artery ratio was known to be associated with the incidence of slow flow^{23,24}, the IVUS-uncrossable group had greater risk of slow flow before RA as compared to the IVUS-crossable group. Moreover, the IVUS-uncrossable group had greater total run time, single run time, rotational speed, and maximum speed reduction during RA as compared to the IVUS-crossable group, which also supports that the lesion complexity was greater in the IVUS-uncrossable group than in the IVUS-crossable group.

The clinical implications of the present study should be noted. First, our study suggests the possibility that the IVUS-crossability can be used as a risk stratification of severe calcified lesions. If the pre-procedural IVUS catheters could not cross the lesion, operators should prepare the occurrence of slow flow after RA. In other words, operators may prepare intracoronary vasodilator such as nitroprusside, intravenous vasopressor such as noradrenaline, or intra-aortic balloon pumping if patient's cardiac function was severely reduced. Moreover, such greater risk should be shared with other staffs such as nurses or medical engineers in the catheter laboratory to perform timely management for slow flow. Second, our results may be useful for establishing an educational program for junior RA operators. Because many literatures regarding RA and imaging devices have been published^{1,3–10}, even junior RA operators may be able to select an appropriate burr size, RotaWire, and RA strategy as long as an imaging device can cross the lesion before RA. However, as we shown here, there were many lesions that an IVUS catheter cannot cross, and the incidence of slow flow was greater in IVUS-uncrossable lesions. Immediate RA to IVUS-uncrossable lesions may be appropriate for senior RA operators, but may not for junior RA operators. We should discuss whether junior RA operators should try immediate RA to such tough lesions or try small balloon dilatation followed by RA to avoid complications. Moreover, as we showed in the multivariate logistic regression analysis, the diffuse long lesion, severe angulation, and initial burr-to-artery ratio were associated with slow flow. Senior RA operators may anticipate the risk of complications from those angiographic findings without IVUS findings, and select small burrs for lesions with small reference diameter to keep appropriate burr-to-artery ratio. However, since those parameters (length, angle, diameter, or ratio) are continuous variables, it would be difficult for junior RA operators to anticipate the risk of complications without established cut-off values. For example, the recommended burr-to-artery ratio varies widely between European Consensus document (0.6) and North American Expert Review (0.4–0.6)^{1,18}. Since the IVUS-crossability is a simple categorical variable (yes/no), it would be easy for junior RA operators to understand the risk of complications. Furthermore, if there were several RA operators in a catheter laboratory, a senior RA operator would actively assist a junior RA operator to perform RA to the IVUS-uncrossable lesion. Those discussions should be incorporated into the educational program for junior RA operators for better patient's outcomes.

Study limitations. Because our study was designed as a single-center, retrospective, observational study, there is a risk of patient selection bias and group-selection bias. Although vessel perforation and burr entrapment are unique complications in RA, our study population was too small to evaluate the difference in those complications between the 2 groups. Since we potentially recognized the greater risk of slow flow in IVUS-uncrossable lesions, we might be more careful to perform RA to IVUS-uncrossable lesions. In fact, we used smaller initial burrs for IVUS-uncrossable lesions. Nevertheless, the incidence of slow flow was greater in IVUS-uncrossable lesions, which supports the strong relationship between slow flow and IVUS-uncrossable lesions. The study endpoint (slow flow) might be influenced by various factors such as settings of power injectors, presence of side holes in guide catheters, and an unblinded evaluator (KS), which would limit reproducibility of the present study. Furthermore, we excluded 158 lesions in which pre-procedural IVUS was not attempted. Although we tended to skip pre-procedural IVUS in our early study period (until 2016), we routinely performed pre-procedural IVUS in our late study period, partly because a dedicated trapping balloon device (Kusabi: KANEKA, Osaka, Japan) facilitated the exchange of guidewires using microcatheters. In the multivariate logistic regression analysis, although we tried to avoid co-linearity of the independent variables, we could not confirm co-linearity of the variables statistically, because the main variable (IVUS-crossability) was a categorical variable (yes/no). Finally, our catheter laboratory rarely used OCT before RA. In fact, of 442 RA lesions during the study period, only 4 lesions (0.9%) received pre-procedural OCT. We decided to exclude those OCT cases from the final study population, because of our limited experiences with OCT.

Conclusion

The incidence of slow flow/severe slow flow just after RA was significantly greater in the IVUS-uncrossable lesions than in the IVUS-crossable lesions. Our study suggests the possibility that the IVUS-crossability can be used as a risk stratification of severe calcified lesions in RA.

Data availability

All data are available from the corresponding author on reasonable request.

Received: 26 February 2020; Accepted: 23 June 2020

Published online: 09 July 2020

References

- Sharma, S. K. *et al.* North American expert review of rotational atherectomy. *Circ. Cardiovasc. Interv.* **12**, e007448. <https://doi.org/10.1161/circinterventions.118.007448> (2019).
- Sakakura, K. *et al.* Incidence and determinants of complications in rotational atherectomy. *Circ. Cardiovasc. Interv.* **9**, e004278. <https://doi.org/10.1161/circinterventions.116.004278> (2016).
- Kim, S. S. *et al.* Intravascular ultrasound assessment of the effects of rotational atherectomy in calcified coronary artery lesions. *Int. J. Cardiovasc. Imaging* **34**, 1365–1371. <https://doi.org/10.1007/s10554-018-1352-y> (2018).
- Maejima, N. *et al.* Relationship between thickness of calcium on optical coherence tomography and crack formation after balloon dilatation in calcified plaque requiring rotational atherectomy. *Circ. J.* **80**, 1413–1419. <https://doi.org/10.1253/circj.CJ-15-1059> (2016).
- De Maria, G. L., Scarsini, R. & Banning, A. P. Management of calcific coronary artery lesions: is it time to change our interventional therapeutic approach?. *JACC Cardiovasc. Interv.* **12**, 1465–1478. <https://doi.org/10.1016/j.jcin.2019.03.038> (2019).
- Amemiya, K. *et al.* Effect of cutting balloon after rotational atherectomy in severely calcified coronary artery lesions as assessed by optical coherence tomography. *Catheter. Cardiovasc. Interv.* **94**, 936–944. <https://doi.org/10.1002/ccd.28278> (2019).
- Kobayashi, N. *et al.* Clinical efficacy of optical coherence tomography-guided versus intravascular ultrasound-guided rotational atherectomy for calcified coronary lesion. *EuroIntervention* <https://doi.org/10.4244/eij-d-19-00725> (2019).
- Dong, H. *et al.* Reappraisal value of a modified rotational atherectomy technique in contemporary coronary angioplasty era. *J. Interv. Cardiol.* <https://doi.org/10.1155/2020/9190702> (2020).
- Mizutani, K. *et al.* Association between debulking area of rotational atherectomy and platform revolution speed-frequency domain optical coherence tomography analysis. *Catheter. Cardiovasc. Interv.* **95**, E1–E7. <https://doi.org/10.1002/ccd.28212> (2020).
- Sakakura, K. *et al.* Intravascular ultrasound enhances the safety of rotational atherectomy. *Cardiovasc. Revasc. Med.* **19**, 286–291. <https://doi.org/10.1016/j.carrev.2017.09.012> (2018).
- Sakakura, K. *et al.* Comparison of complications with a 1.25-mm versus a 1.5-mm burr for severely calcified lesions that could not be crossed by an intravascular ultrasound catheter. *Cardiovasc. Interv. Ther.* <https://doi.org/10.1007/s12928-019-00606-9> (2019).
- Sakakura, K. *et al.* Comparison of frequency of complications with on-label versus off-label use of rotational atherectomy. *Am. J. Cardiol.* **110**, 498–501. <https://doi.org/10.1016/j.amjcard.2012.04.021> (2012).
- Sakakura, K. *et al.* The incidence of slow flow after rotational atherectomy of calcified coronary arteries: a randomized study of low speed versus high speed. *Catheter. Cardiovasc. Interv.* **89**, 832–840. <https://doi.org/10.1002/ccd.26698> (2017).
- Sakakura, K. *et al.* Beta-blocker use is not associated with slow flow during rotational atherectomy. *J. Invasive Cardiol.* **24**, 379–384 (2012).
- Yamamoto, K. *et al.* Determinants of Greater Peak radiation skin dose in percutaneous coronary intervention for chronic total occlusion. *J. Cardiol.* <https://doi.org/10.1016/j.jjcc.2020.02.021> (2020).
- Sakakura, K. *et al.* Association of excessive speed reduction with clinical factors during rotational atherectomy. *Cardiovasc. Revasc. Med.* <https://doi.org/10.1016/j.carrev.2019.05.014> (2019).
- Matsuo, H. *et al.* Prevention of no-reflow/slow-flow phenomenon during rotational atherectomy—a prospective randomized study comparing intracoronary continuous infusion of verapamil and nicorandil. *Am. Heart J.* **154**(994), e991–996. <https://doi.org/10.1016/j.ahj.2007.07.036> (2007).
- Barbato, E. *et al.* European expert consensus on rotational atherectomy. *EuroIntervention* **11**, 30–36. <https://doi.org/10.4244/eijv11i1a6> (2015).
- Yamamoto, K. *et al.* Trapping balloon technique for removal of the burr in rotational atherectomy. *Int. Heart J.* **59**, 399–402. <https://doi.org/10.1536/ihj.17-359> (2018).
- Yamamoto, K. *et al.* Comparison of clinical outcomes between sufficient versus insufficient diagonal branch flow in anterior acute myocardial infarction. *Heart Vessels* **34**, 1096–1103. <https://doi.org/10.1007/s00380-019-01343-y> (2019).
- Levey, A. S. *et al.* Using standardized serum creatinine values in the modification of diet in renal disease study equation for estimating glomerular filtration rate. *Ann. Intern. Med.* **145**, 247–254 (2006).
- Desai, R. *et al.* Modern-day nationwide utilization of intravascular ultrasound and its impact on the outcomes of percutaneous coronary intervention with coronary atherectomy in the United States. *J. Ultrasound Med.* **38**, 2295–2304. <https://doi.org/10.1002/jum.14922> (2019).
- Sharma, S. K. *et al.* Risk factors for the development of slow flow during rotational coronary atherectomy. *Am. J. Cardiol.* **80**, 219–222 (1997).
- Sardella, G., De Luca, L., Adorisio, R., Di Russo, C. & Fedele, F. Effects of rotational atherectomy with a reduced burr-to-artery ratio on coronary no-reflow. *Minerva Cardioangiol.* **52**, 209–217 (2004).

Acknowledgements

The authors acknowledge Ryo Kokubo, M.E.; Kohei Matsuda, M.E.; and all staff in the catheter laboratory in Jichi Medical University, Saitama Medical Center for their technical support in this study. Funding: This work was supported by Grants-in-Aid for Scientific Research (C) (Kenichi Sakakura, JSPS KAKENHI Grant Number 17K09521).

Author contributions

K.S. conceived the idea of the study. K.S., Y.T., K.Y., T.T., M.S., and H.W. collected the data. K.S. performed statistical analysis, and drafted a manuscript. S.M. and H.F. interpreted the data. All authors commented on the manuscript and approved the final version.

Competing interests

Dr. Sakakura has received speaking honoraria from Abbott Vascular, Boston Scientific, Medtronic Cardiovascular, Terumo, OrbusNeich, Japan Lifeline, Kaneka, and NIPRO; he has served as a proctor for Rotablator for Boston Scientific, and he has served as a consultant for Abbott Vascular and Boston Scientific. Prof. Fujita has served as a consultant for Mehergen Group Holdings, Inc. Other authors have no conflicts of interest to declare.

Additional information

Correspondence and requests for materials should be addressed to K.S.

Reprints and permissions information is available at www.nature.com/reprints.

Publisher's note Springer Nature remains neutral with regard to jurisdictional claims in published maps and institutional affiliations.



Open Access This article is licensed under a Creative Commons Attribution 4.0 International License, which permits use, sharing, adaptation, distribution and reproduction in any medium or format, as long as you give appropriate credit to the original author(s) and the source, provide a link to the Creative Commons license, and indicate if changes were made. The images or other third party material in this article are included in the article's Creative Commons license, unless indicated otherwise in a credit line to the material. If material is not included in the article's Creative Commons license and your intended use is not permitted by statutory regulation or exceeds the permitted use, you will need to obtain permission directly from the copyright holder. To view a copy of this license, visit <http://creativecommons.org/licenses/by/4.0/>.

© The Author(s) 2020